Cell Metabolism, Volume *33*

Supplemental information

Exercise-induced angiogenesis is dependent on metabolically primed ATF3/4^{+} endothelial cells

Zheng Fan, Guillermo Turiel, Raphaela Ardicoglu, Moheb Ghobrial, Evi Masschelein, Tea Kocijan, Jing Zhang, Ge Tan, Gillian Fitzgerald, Tatiane Gorski, Abdiel Alvarado-Diaz, Paola Gilardoni, Christopher M. Adams, Bart Ghesquière, and Katrien De Bock

SUPPLEMENTAL INFORMATION

Table S1. Sequences of primers used for RT-PCR. Related to Figure 4, S2, S3, S4, S6.

gene	Forward	Reverse
18s (Mm.& Hs.)	AGTCCCTGCCCTTTGTACACA	CGATCCGAGGGCCTCACTA
Atf4 (Mm.)	CAACCTATAAAGGCTTGCGG	CTGCTGGATTTCGTGAAGAG
ATF4 (Hs.)	GTTCTCCAGCGACAAGGCTA	ATCCTGCTTGCTGTTGTTGG
Atf3 (Mm.)	GGAGATGTCAGTCACCAAGTC	TTTCTCTGACTCTTTCTGCAGG
ATF3 (Hs.)	GCGACGAGAAAGAAATAAGATTGC	GCTTCTCCGACTCTTTCTGC
Fos (Mm.)	CAAAGTAGAGCAGCTATCTCCT	CAAGTTGATCTGTCTCCGCT
FOS (Hs.)	CAAGGTGGAACAGTTATCTCCAG	GAGTGTATCAGTCAGCTCCCT
Junb (Mm.)	CGACCTGCACAAGATGAACC	GAGTAACTGCTGAGGTTGGTG
JUNB (Hs.)	CGATCTGCACAAGATGAACCA	GTTGGTGTAAACGGGAGGTG
Fosb (Mm.)	CCCGAGAAGAGACACTTACC	GATCAGTTTCCGCCTGAAGTC
FOSB (Hs.)	GGAACGAAATAAACTAGCAGCAG	CTCCAACTGATCTGTCTCCG
Jun (Mm.)	CAAACTTTGTTACAGAAGCGGG	CATCTTTGCAGTCATAGAACGG
JUN (Hs.)	ACCTTCTATGACGATGCCCTC	GCTCTGTTTCAGGATCTTGGG
PDK1 (Hs.)	TCTCAGGACACCATCCGTTCA	ACCATGTTCTTCTAGGCCTTTCAT
PDK4 (Hs.)	GTAGCAGTGGTCCAAGATGCC	ACACGATGTGAATTGGTTGGTCT
ANG2 (Hs.)	TGCCACGGTGAATAATTCAG	TTCTTCTTTAGCAACAGTGGG
MXI1 (Hs.)	GCCAAAGCACACATCAAGAAACT	GCTGTTCCAGTCGCCACTTT
HEY1 (Hs.)	TGGATCACCTGAAAATGCTGC	CGAAATCCCAAACTCCGATAGT
HES1 (Hs.)	TGAAGAAAGATAGCTCGCGGC	GGTACTTCCCCAGCACACTT
DLL4 (Hs.)	AGGCCTGTTTTGTGACCAAG	CTCCAGCTCACAGTCCACAC
NRARP (Hs.)	CGCTGTTGCTGGTGTTCTAAA	CATTGACCACGCAGTGTTTTC
cMYC (Hs.)	TCCTCGGATTCTCTGCTCTC	TCTTGTTCCTCCTCAGAGTCG
CDK4 (Hs.)	CCATCAGCACAGTTCGTGAGGT	TCAGTTCGGGATGTGGCACAGA
CCND2 (Hs.)	GAGAAGCTGTCTCTGATCCGCA	CTTCCAGTTGCGATCATCGACG
CCNB2 (Hs.)	CAACCAGAGCAGCACAAGTAGC	GGAGCCAACTTTTCCATCTGTAC
Psat1 (Mm.)	TGTGCTCGAAATGAGTCACAG	CCACCTCCTTGTACAAAGATCAC
PSAT1 (Hs.)	GGTGATTGTCCGTGATGACC	ATGACGTAGATGCTGAAACATGG
Phgdh (Mm.)	GGTTACACAAGGAACATCTCTG	CTTAGCGTTCACCAAGTTCAC
PHGDH (Hs.)	AAGGGCATCTTGGTTATGAACAC	TCCCATGAACTTCTTCCGCT
Psph (Mm.)	GTGGGAAAGGAAAGGTTATTCGG	CCAATGAAAGCATCAGCAGGA
PSPH (Hs.)	CCAACAGCTGAATCTGGTGG	AATGAAAGCATCAGCAGGAGG

Slc1a5 (Mm.)	TCTGCCTCTCATCTACTTCCTC	CACACCATTCTTCTCCTCTACAC
SLC1A5 (Hs.)	CCTTTCGCTCATACTCTACCAC	AGACGATGGCAAACACTACC
Slc1a4 (Mm.)	ACCTCATCCGATTCTTCAATTCC	TCTACAATCTTGCTTCCGATCAG
SLC1A4 (Hs.)	TTTGCTCTGGTGTTAGGAGTG	GTCGCTGAGCACATAATCCA
Asns (Mm.)	AAGCGAGCATCATGAAGTCC	AATACATGCCCACAGATGCC
ASNS (Hs.)	TTTCACAAGGCTCCTTCTCC	AAATGGGACTCTCAGTTCAAGAC
Slc7a1 (Mm.)	AGTCTTACAGCAGATTCGCTC	GGTCATAGGTGTTGAGGCAG
SLC7A1 (Hs.)	GGCTCAGCTTACCTCTACAG	CTTGAAGTACCGATGATGTAGGA
Slc7a5 (Mm.)	CTCTTCCTCATTGCCGTGTC	CCGTCACAGAGAAGATAGCC
SLC7A5 (Hs.)	AGATCGGGAAGGGTGATGTG	AAGTAATTCCATCCTCCATAGGC
Shmt2 (Mm.)	AGAGGGAGAAGGACAGACAG	TCCTCCGTAGTATCTCTTGCC
SHMT2 (Hs.)	CCTCAGAGAACTTCTGCAGC	CCCATAGTATCTCTTGCCAGGA
Apold1 (Mm.)	CCTGGAGGCCAGAGTGAA	CCAGCAGCAATCCTTGGAA
Egr1 (Mm.)	TATGAGCACCTGACCACAGAG	GTTTGGCTGGGATAACTCGTC
Zfp36 (Mm.)	CCATCTACGAGAGCCTCCAG	TCCGAGTTTATGTTCCAAAGTCC
Dusp1 (Mm.)	TCAGCCAATTGTCCTAACCA	CCTTGATGGAGTCTATGAAGTC
Egr4 (Mm.)	GACTTAACAGACTCCTGCTTCC	GCCAGACATGAGGTTGAAGAG
Nr4a1 (Mm.)	TTCTTCAAGCGCACAGTACAG	GTCCGTACAACTTCCTTCACC
Nr4a3 (Mm.)	TAGACTTTCCATCAGGTCAAACAC	CCAAATCCTCGAAGGCACTG

Homo sapiens: : (Hs.); Mus musculus: (Mm.).

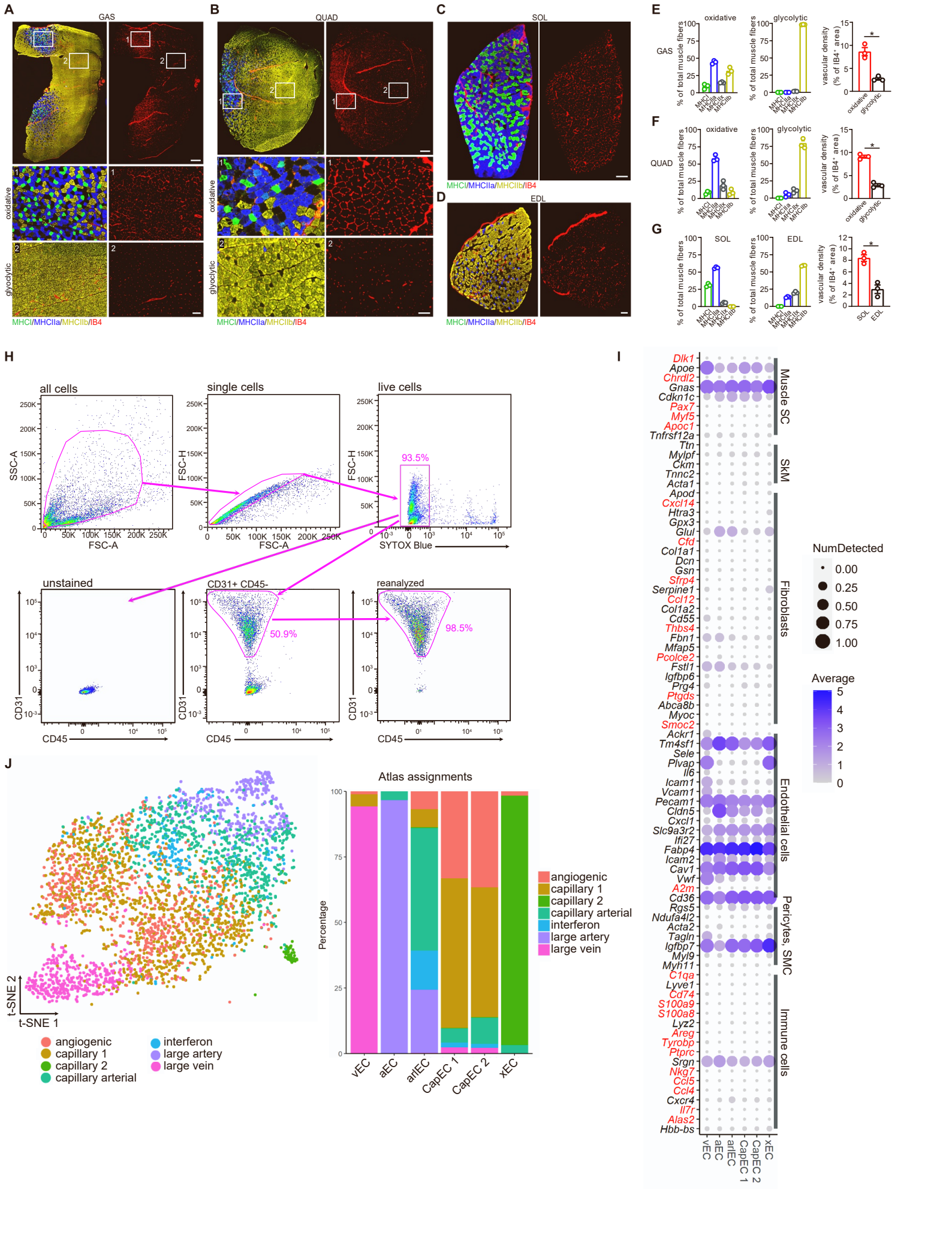
A
GAS
oxidative
glycolytic
MHCI/MHCIIa/MHCIIb/IB4
B
QUAD
oxidative
glycolytic
MHCI/MHCIIa/MHCIIb/IB4
C
SOL
MHCI/MHCIIa/MHCIIb/IB4
D
EDL
MHCI/MHCIIa/MHCIIb/IB4
E
GAS
oxidative
glycolytic
% of total muscle fibers
MHCI
MHCIIa
MHCIIx
MHCIIb
vascular density (% of IB4+ area)
F
QUAD
G
SOL
EDL
H
all cells
single cells
live cells
SSC-A
FSC-A
FSC-H
SYTOX Blue
93.5%
unstained
CD31+ CD45-
reanalyzed
CD31
CD45
50.9%
98.5%
I
Dlk1
Apoe
Chrdl2
Gnas
Cdkn1c
Pax7
Myf5
Apoc1
Tnfrsf12a
Ttn
Mylpf
Ckm
Tnnc2
Acta1
Apod
Cxcl14
Htra3
Gpx3
Glul
Cfd
Col1a1
Dcn
Gsn
Sfrp4
Serpine1
Ccl12
Col1a2
Cd55
Thbs4
Fbn1
Mfap5
Pcolce2
Fstl1
Igfbp6
Prg4
Ptgds
Abca8b
Myoc
Smoc2
Ackr1
Tm4sf1
Sele
Plvap
Il6
Icam1
Vcam1
Pecam1
Cldn5
Cxcl1
Slc9a3r2
Ifi27
Fabp4
Icam2
Cav1
Vwf
A2m
Cd36
Rgs5
Ndufa4l2
Acta2
Tagln
Igfbp7
Myl9
Myh11
C1qa
Lyve1
Cd74
S100a9
S100a8
Lyz2
Areg
Tyrobp
Ptprc
Srgn
Nkg7
Ccl5
Ccl4
Cxcr4
Il7r
Alas2
Hbb-bs
Muscle SC
SkM
Fibroblasts
Endothelial cells
Pericytes, SMC
Immune cells
vEC
aEC
arlEC
CapEC 1
CapEC 2
xEC
NumDetected
0.00
0.25
0.50
0.75
1.00
Average
J
t-SNE 1
t-SNE 2
angiogenic
capillary 1
capillary 2
capillary arterial
interferon
large artery
large vein
Atlas assignments
Percentage
vEC
aEC
arlEC
CapEC 1
CapEC 2
xEC

Figure S1. scRNA-seq reveals endothelial cell subpopulations in skeletal muscle. Related to Figure 1.

(**A-D**) Representative fluorescence images of IB4 (red) combined with type I (MHCI, green), type IIa (MHCIIa, blue) and type IIb (MHCIIb, yellow) fiber type staining in m. gastrocnemius (GAS) (A), m. quadriceps (QUAD) (B), m. soleus (SOL) (C) and m. extensor digitorum longus (EDL) (D). Scale bar, 500 μm. (**E-G**) Quantification of fiber types and vessel density (% of $IB4^+$ area) in oxidative and glycolytic areas of GAS (E), QUAD (F), SOL and EDL (G). (**H**) Gating strategy for isolation of mECs by FACS and analysis of unstained, CD31+CD45 stained samples and re-analysis of purified mECs. (**I**) Dot-plot showing marker genes expression of common cell types found in skeletal muscle in the EC populations. Genes in red were filtered out during pre-processing analysis due to low expression (expressed in less than 3 cells). (**J**) Left, t-SNE plot of EC populations colored based on the unbiased mapping to Kalucka et al., 2020. Right, bar plots showing the percentage of each mapping assignment in the EC populations. Student's *t* test (two-tailed, unpaired) in **E, F, G,** (*$p<0.05$). Bar graphs represent mean ± SEM.

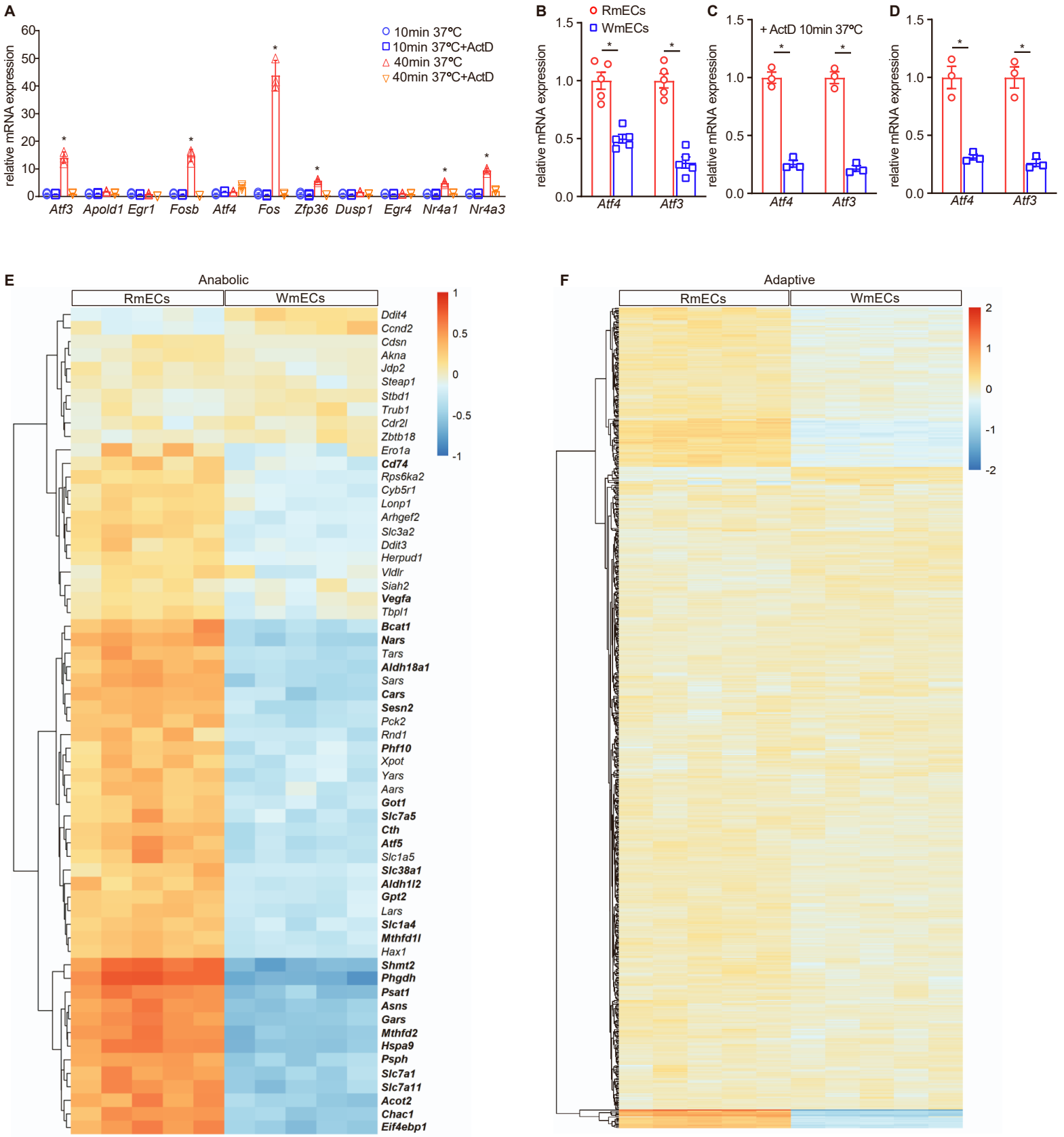
A
relative mRNA expression
10min 37°C
10min 37°C+ActD
40min 37°C
40min 37°C+ActD
Atf3
Apold1
Egr1
Fosb
Atf4
Fos
Zfp36
Dusp1
Egr4
Nr4a1
Nr4a3
B
RmECs
WmECs
Atf4
Atf3
C
+ ActD 10min 37°C
D
E
Anabolic
RmECs
WmECs
Ddit4
Ccnd2
Cdsn
Akna
Jdp2
Steap1
Stbd1
Trub1
Cdr2l
Zbtb18
Ero1a
Cd74
Rps6ka2
Cyb5r1
Lonp1
Arhgef2
Slc3a2
Ddit3
Herpud1
Vldlr
Siah2
Vegfa
Tbpl1
Bcat1
Nars
Tars
Aldh18a1
Sars
Cars
Sesn2
Pck2
Rnd1
Phf10
Xpot
Yars
Aars
Got1
Slc7a5
Cth
Atf5
Slc1a5
Slc38a1
Aldh1l2
Gpt2
Lars
Slc1a4
Mthfd1l
Hax1
Shmt2
Phgdh
Psat1
Asns
Gars
Mthfd2
Hspa9
Psph
Slc7a1
Slc7a11
Acot2
Chac1
Eif4ebp1
F
Adaptive
RmECs
WmECs

Figure S2. Muscle contains two capillary EC populations characterized by distinct *Atf3/4*. Related to Figure 2.

(**A**) RNA analysis of IEGs in mECs isolated by different dissociation procedures (n=3). (**B**) qRT-PCR Validation of *Atf3* and *Atf4* expression in RmECs and WmECs isolated for RNA sequencing (n=5). (**C**) RNA analysis of *Atf3* and *Atf4* by qRT-PCR in RmECs and WmECs isolated using 10 min digestion (37°C) protocol in the presence of ActD (n=3). (**D**) RNA analysis of *Atf3* and *Atf4* by qRT-PCR in 7 days cultured RmECs and WmECs (n=3). (**E**) Heatmap showing relative expression of ATF4-dependent anabolic gene set (Torrence et al., 2021) in RmECs versus WmECs. Bold gene names refer to differentially expressed genes between RmECs and WmECs (log fold change > 1 and adjusted p-value < 0.05). (**F**) Heatmap showing relative expression of ATF4-dependent adaptative gene set (Torrence et al., 2021) in RmECs versus WmECs. Student's *t* test (two-tailed, unpaired) in **A**, **B**, **C** and **D** (*p<0.05). n.s.: not significant. Bar graphs represent mean ± SEM.

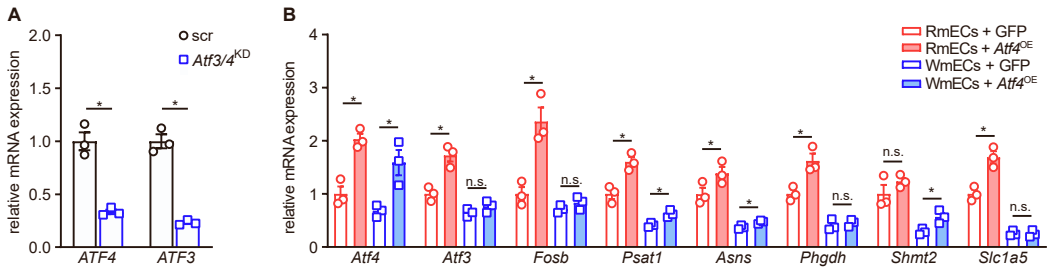

Figure S3. ATF3/4^{low} WmECs have a lower angiogenic potential. Related to Figure 3.

(**A**) Gene knock down validation of *Atf3* and *Atf4* by qRT-PCR in WT (scr) and *Atf3/4*^{KD} HUVECs (n=3). (**B**) Gene profiling by qRT-PCR of RmECs versus WmECs either or not combined with overexpression of *Atf4* (doxycycline inducible, 24hours) (n=3). Student's *t* test (two-tailed, unpaired) (*p<0.05). n.s.: not significant. Bar graphs represent mean ± SEM.

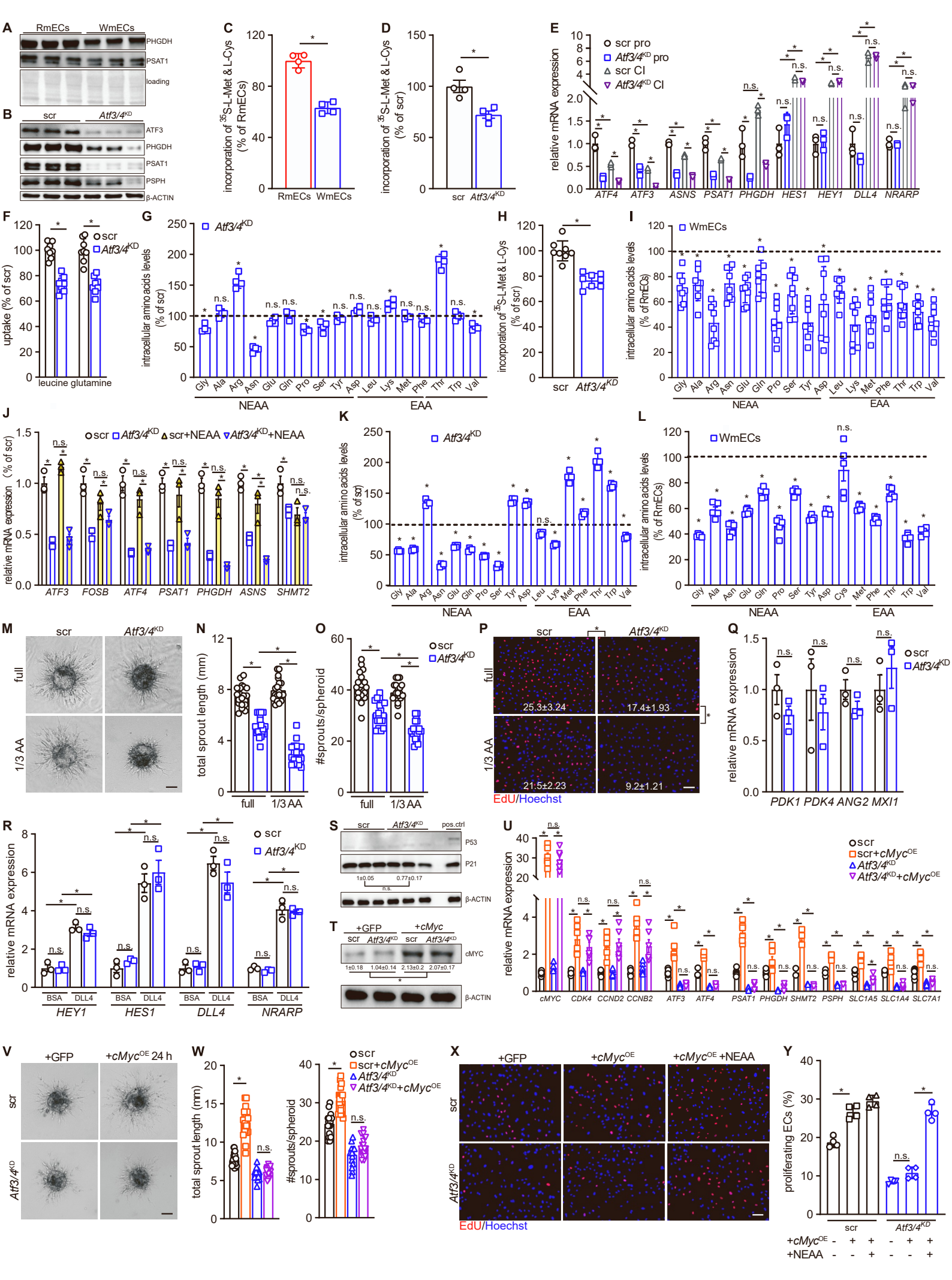
A
RmECs
WmECs
PHGDH
PSAT1
loading
B
scr
Atf3/4KD
ATF3
PHGDH
PSAT1
PSPH
β-ACTIN
C
incorporation of 35S-L-Met & L-Cys (% of RmECs)
RmECs
WmECs
D
incorporation of 35S-L-Met & L-Cys (% of scr)
scr
Atf3/4KD
E
relative mRNA expression
scr pro
Atf3/4KD pro
scr CI
Atf3/4KD CI
ATF4
ATF3
ASNS
PSAT1
PHGDH
HES1
HEY1
DLL4
NRARP
F
uptake (% of scr)
scr
Atf3/4KD
leucine
glutamine
G
Atf3/4KD
intracellular amino acids levels (% of scr)
Gly Ala Arg Asn Glu Gln Pro Ser Tyr Asp Leu Lys Met Phe Thr Trp Val
NEAA
EAA
H
incorporation of 35S-L-Met & L-Cys (% of scr)
scr
Atf3/4KD
I
WmECs
intracellular amino acids levels (% of RmECs)
Gly Ala Arg Asn Glu Gln Pro Ser Tyr Asp Leu Lys Met Phe Thr Trp Val
NEAA
EAA
J
scr
Atf3/4KD
scr+NEAA
Atf3/4KD+NEAA
relative mRNA expression (% of scr)
ATF3
FOSB
ATF4
PSAT1
PHGDH
ASNS
SHMT2
K
Atf3/4KD
intracellular amino acids levels (% of scr)
Gly Ala Arg Asn Glu Gln Pro Ser Tyr Asp Leu Lys Met Phe Thr Trp Val
NEAA
EAA
L
WmECs
intracellular amino acids levels (% of RmECs)
Gly Ala Asn Glu Gln Pro Ser Tyr Asp Cys Met Phe Thr Trp Val
NEAA
EAA
M
scr
Atf3/4KD
full
1/3 AA
N
total sprout length (mm)
full
1/3 AA
O
scr
Atf3/4KD
#sprouts/spheroid
full
1/3 AA
P
scr
Atf3/4KD
full
1/3 AA
25.3±3.24
17.4±1.93
21.5±2.23
9.2±1.21
EdU/Hoechst
Q
scr
Atf3/4KD
relative mRNA expression
PDK1 PDK4 ANG2 MXI1
R
scr
Atf3/4KD
relative mRNA expression
BSA
DLL4
HEY1
HES1
DLL4
NRARP
S
scr
Atf3/4KD
pos.ctrl
P53
P21
1±0.05
0.77±0.17
β-ACTIN
T
+GFP
+cMyc
scr
Atf3/4KD
cMYC
1±0.18
1.04±0.14
2.13±0.2
2.07±0.17
β-ACTIN
U
scr
scr+cMycOE
Atf3/4KD
Atf3/4KD+cMycOE
relative mRNA expression
cMYC
CDK4
CCND2
CCNB2
ATF3
ATF4
PSAT1
PHGDH
SHMT2
PSPH
SLC1A5
SLC1A4
SLC7A1
V
+GFP
+cMycOE 24 h
scr
Atf3/4KD
W
scr
scr+cMycOE
Atf3/4KD
Atf3/4KD+cMycOE
total sprout length (mm)
#sprouts/spheroid
X
+GFP
+cMycOE
+cMycOE +NEAA
scr
Atf3/4KD
EdU/Hoechst
Y
proliferating ECs (%)
scr
Atf3/4KD
+cMycOE
+NEAA

Figure S4. ATF3/4 rewires amino acid metabolism and biomass synthesis to metabolically prime RmECs for angiogenesis. Related to Figure 4.

(**A, B**) Representative image of Western Blot of enzymes involved in *de novo* serine biosynthesis in RmECs versus WmECs (A), as well as in WT (scr) versus *Atf3/4*^{KD} HUVECs (B). Total protein loading or β-actin was used as loading control (n=3). (**C**, **D**) Protein synthesis rate measured by incorporation of radioactive amino acid mix (^{35}S-L-methionine and ^{35}S-L-cysteine) in RmECs versus WmECs (C) as well as WT (scr) versus *Atf3/4*^{KD} HUVECs (D) (n=4). (**E**) Gene profiling by qRT-PCR of WT (scr) versus *Atf3/4*^{KD} HUVECs in proliferative (pro) and contact inhibited (CI) conditions (n=3). (**F**) Leucine and glutamine uptake assay in WT (scr) and *Atf3/4*^{KD} HUVECs under CI conditions (n=8). (**G**) Intracellular free amino acids abundance measurement by LC-MS in WT (scr) versus *Atf3/4*^{KD} HUVECs cultured in full medium under CI condition (n=4). (**H**) Protein synthesis rate measured by incorporation of radioactive amino acid mix (^{35}S-L-methionine and ^{35}S-L-cysteine) in WT (scr) versus *Atf3/4*^{KD} HUVECs under CI condition (n=8). (**I**) Intracellular free amino acids abundance measurement by LC-MS in immediately lysed primary RmECs versus WmECs isolated by CD31 pluri-beads (n=8). (**J**) Gene profiling by qRT-PCR of WT (scr) versus *Atf3/4*^{KD} HUVECs treated with or without nonessential amino acids (NEAA) (n=3). (**K**, **L**) Intracellular free amino acids abundance measurement by LC-MS in WT (scr) versus *Atf3/4*^{KD} HUVECs (K) as well as RmECs versus WmECs (L) cultured in reduced amino acids (1/3 AA) medium (n=4-5). (**M**) Representative pictures and (**O**) quantifications of sprouting WT (scr) and *Atf3/4*^{KD} HUVEC spheroids in full amino acid (full) conditions and reduced amino acid (1/3 AA)(n=30). Scale bar, 50 μm. (**P**) Representative fluorescence images of EdU incorporation in WT (scr) and *Atf3/4*^{KD} HUVECs cultured in full amino acids conditions (full) and 1/3 AA conditions. Scale bar, 100 μm. Numbers within images indicate the percentage quantification of proliferating ECs (EdU^{+} nucleus) in total Hoechst^{+} nucleus (mean ± SEM) (n=6). (**Q**) Gene expression analysis of FOXO1 target genes in WT (scr) and *Atf3/4*^{KD} HUVECs (n=3). (**R**) Gene expression analysis of NOTCH target genes upon stimulation with the NOTCH ligand DLL4 in WT (scr) and *Atf3/4*^{KD} HUVECs (n=3). (**S**) Representative image of Western Blot of P53 and P21 in WT (scr) and *Atf3/4*^{KD} HUVECs. β-actin was used as loading control, numbers below the blot indicate the quantification of P21 blot (P53 was not detected) (n=3). Mitomycin C treated HUVECs

were used as positive control. (**T**) Representative image of Western Blot of cMyc in WT (scr) and *Atf3/4*^{KD} HUVECs either or not combined with overexpression of *cMyc.* β-actin was used as loading control (n=3). (**U**) Gene expression analysis on cMYC target genes in WT (scr) and *Atf3/4*^{KD} HUVECs either or not combined with overexpression of *cMyc* (n=3-6). (**V, W**) Representative images (V) and quantification (W) of total sprout length and number of sprouts in scr versus *Atf3/4*^{KD} HUVECs either or not combined with overexpression of *cMyc* (n=20). Scale bar, 50 μm. (**X**) Representative fluorescence images of EdU incorporation in WT (scr) and *Atf3/4*^{KD} HUVECs either or not combined with overexpression of cMyc. Cells were cultured in low mitogenic condition (1/3 AA and 1/3 growth factors) or supplemented with nonessential amino acids (+NEAA). Scale bar, 100 μm. (**Y**) Percentage quantification of proliferating ECs (EdU^{+} nucleus) in total Hoechst^{+} nucleus (n=4). Student's *t* test (two-tailed, unpaired) in **C**, **D**, **F**, **G**, **H**, **I**, **K**, **L**, **Q**, **S**(*p<0.05). One-way ANOVA with Tukey's multiple comparisons test in **O, T, W** (*p<0.05). Two-way ANOVA with Sidak's multiple comparisons test in **E, J, R, U, Y** (*p<0.05). n.s.: not significant. Bar graphs represent mean ± SEM.

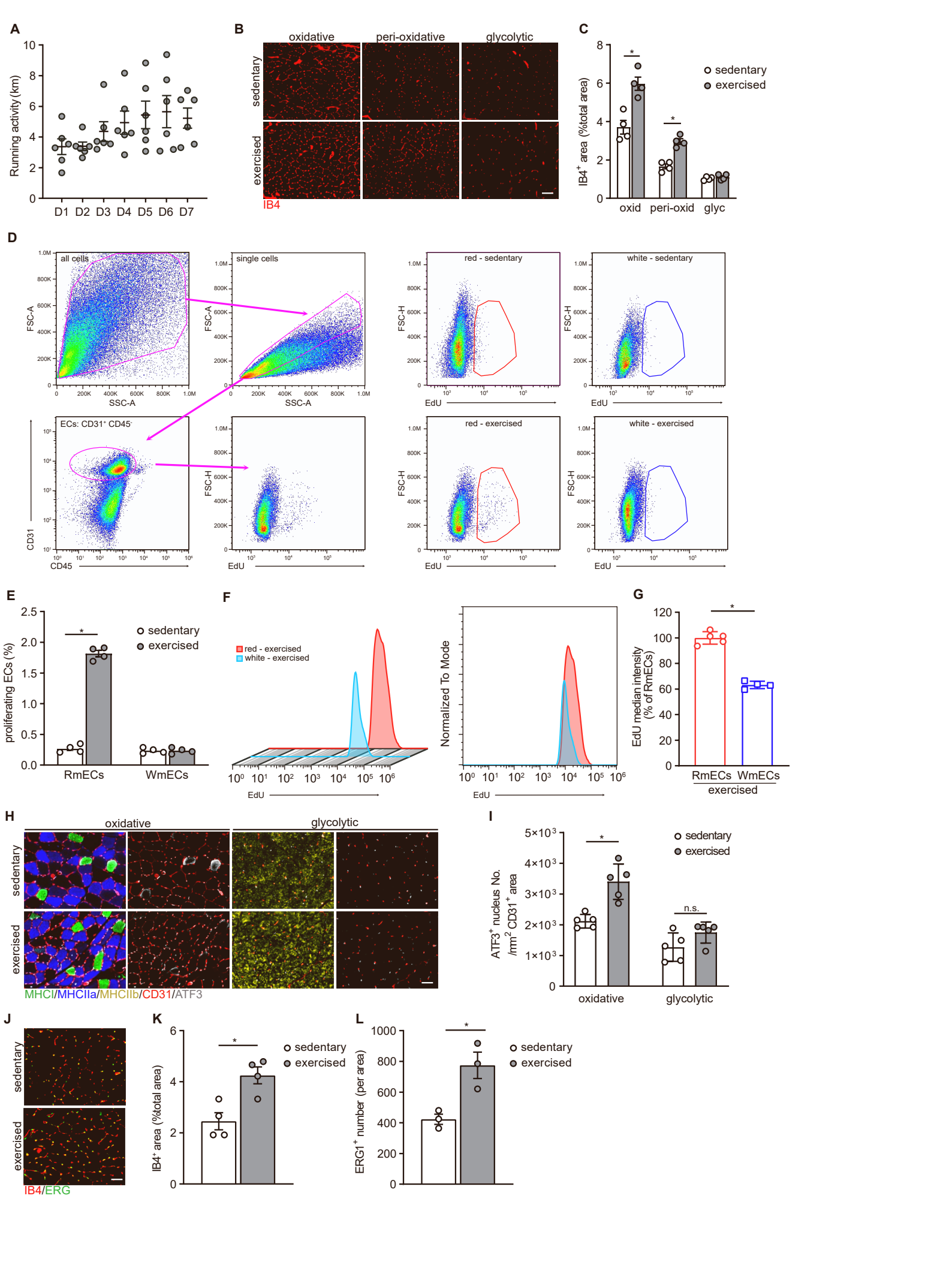
A
Running activity (km)
D1 D2 D3 D4 D5 D6 D7
B
oxidative
peri-oxidative
glycolytic
sedentary
exercised
IB4
C
IB4+ area (%total area)
oxid
peri-oxid
glyc
sedentary
exercised
D
all cells
single cells
red - sedentary
white - sedentary
red - exercised
white - exercised
ECs: CD31+ CD45-
FSC-A
SSC-A
FSC-H
CD31
CD45
EdU
E
proliferating ECs (%)
RmECs
WmECs
sedentary
exercised
F
red - exercised
white - exercised
Normalized To Mode
EdU
G
EdU median intensity (% of RmECs)
RmECs
WmECs
exercised
H
oxidative
glycolytic
sedentary
exercised
MHCI/MHCIIa/MHCIIb/CD31/ATF3
I
ATF3+ nucleus No. /mm2 CD31+ area
sedentary
exercised
n.s.
oxidative
glycolytic
J
sedentary
exercised
IB4/ERG
K
IB4+ area (%total area)
sedentary
exercised
L
ERG1+ number (per area)
sedentary
exercised

Figure S5. Exercise leads to a selective expansion of RmECs. Related to Figure 5.

(**A**) Running activity (km/ dark phase) measured by TSE running wheel systems for the first 7 days, D: dark phase. (**B, C**) Representative images of IB4 stainings (B) and quantification of $IB4^+$ area (% of total area) (C) in oxidative, peri-oxidative and glycolytic areas of GAS from sedentary versus exercised (14 days voluntary running) mice. Scale bar, 100 µm. (n=4). (**D**) Gating strategy for proliferating endothelial cell ($CD31^+$ $CD45^-$ EdU^+) isolated from different areas of sedentary and exercised muscle. (**E**) Quantification of proliferating endothelial cells ($CD31^+$ $CD45^-$ EdU^+) in red oxidative and white glycolytic muscle from sedentary versus exercised mice (n=4). (**F, G**) Histogram of EdU intensity comparison (F) and quantification (G) of RmECs and WmECs *in vivo* after exercise. (**H**) Representative fluorescence images showing ATF3 (grey) and CD31 (red) combined with type I (MHCI, green), type IIa (MHCIIa, blue) and type IIb (MHCIIb, yellow) fiber type staining in oxidative and glycolytic areas of m. quadriceps isolated from sedentary versus 14 days voluntary exercised mice. Scale bar, 50 µm. (**I**) Quantification of the percentage of $ATF3^+$ vessels in oxidative and glycolytic areas of sedentary and exercised quadriceps muscle (n=5). (**J, K, L**) Representative images (J) and quantifications (K) of IB4 ($IB4^+$ area) (% of total area) and ERG number per area (L) in peri-oxidative area of sedentary versus exercised (14 days voluntary running) mice (n=3-4). Scale bar, 100 µm. Student's *t* test (two-tailed, unpaired) in **C, E, K, L** (*$p<0.05$). One-way ANOVA with Tukey's multiple comparisons test in **I** (*$p<0.05$). n.s.: not significant. Each dot represents a single mouse (**A, C, E, G, I, K, L**). Bar graphs represent mean ± SEM.

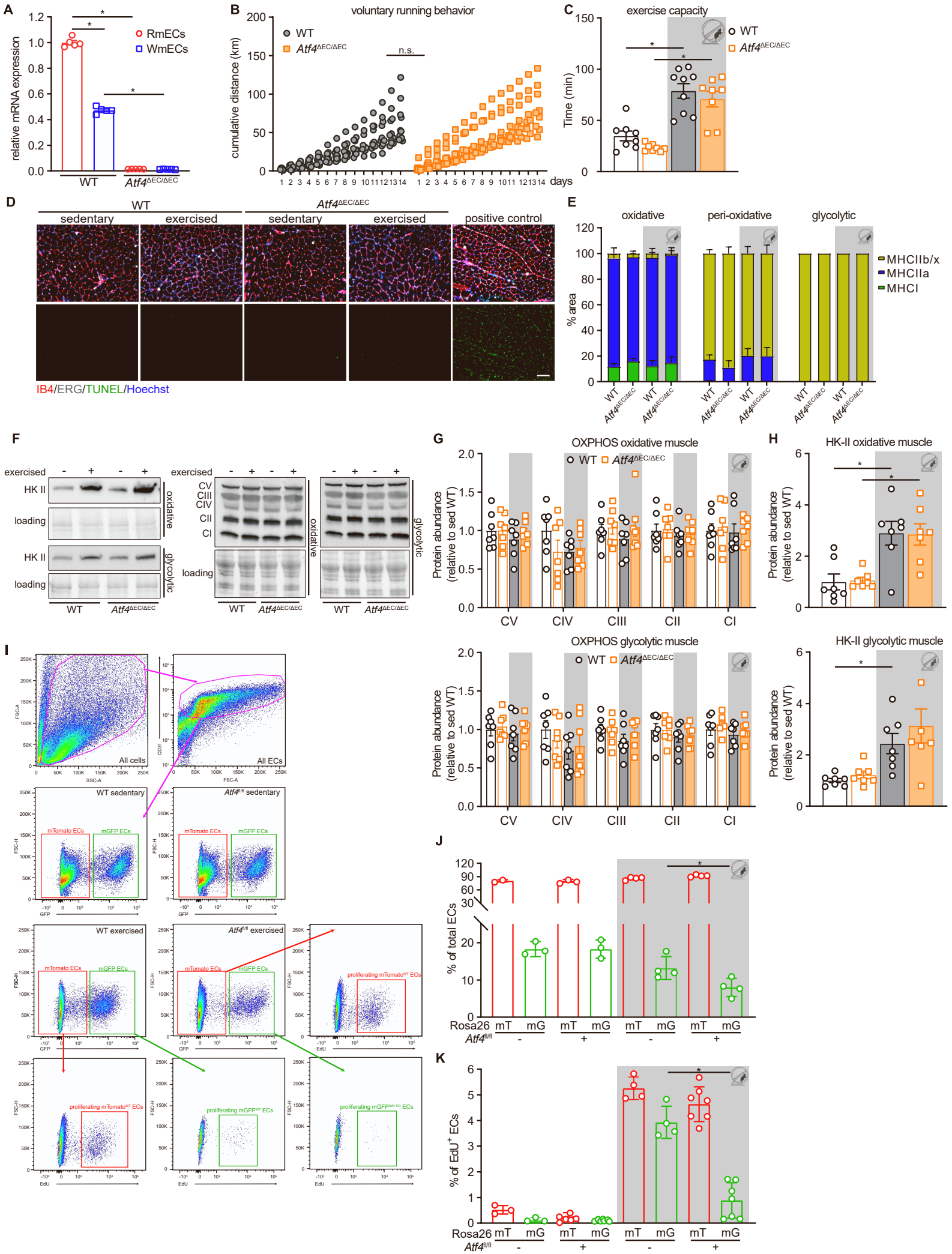
A
relative mRNA expression
RmECs
WmECs
WT
Atf4ΔEC/ΔEC
B
voluntary running behavior
cumulative distance (km)
WT
Atf4ΔEC/ΔEC
n.s.
days
C
exercise capacity
Time (min)
WT
Atf4ΔEC/ΔEC
D
WT
Atf4ΔEC/ΔEC
sedentary
exercised
sedentary
exercised
positive control
IB4/ERG/TUNEL/Hoechst
E
oxidative
peri-oxidative
glycolytic
% area
MHCIIb/x
MHCIIa
MHCI
F
exercised
HK II
loading
oxidative
glycolytic
CV
CIII
CIV
CII
CI
G
OXPHOS oxidative muscle
Protein abundance (relative to sed WT)
CV
CIV
CIII
CII
CI
OXPHOS glycolytic muscle
H
HK-II oxidative muscle
HK-II glycolytic muscle
I
All cells
All ECs
WT sedentary
Atf4fl/fl sedentary
mTomato ECs
mGFP ECs
WT exercised
Atf4fl/fl exercised
proliferating mTomatoWT ECs
proliferating mGFPWT ECs
proliferating mGFPΔEC KO ECs
J
% of total ECs
Rosa26
mT
mG
Atf4fl/fl
K
% of EdU+ ECs

Figure S6. Deletion of *Atf4* in ECs impairs exercise induced endothelial proliferation and vascular expansion. Related to Figure 6.

(**A**) Validation of *Atf4* homozygous knock out in FACS sorted mECs isolated from WT and *Atf4*$^{\Delta EC/\Delta EC}$ mice (n=5). (**B**) Running activity (km/ dark phase) of WT and *Atf4*$^{\Delta EC/\Delta EC}$ mice measured by TSE running wheel systems for 14 days. (**C**) Aerobic exercise capacity test of WT and *Atf4*$^{\Delta EC/\Delta EC}$ mice with treadmill system. Aerobic capacity is expressed as total running time during the test (n=8-9). (**D**) Representative fluorescence images showing apoptotic nucleus (TUNEL staining, green) in cryosections of WT and *Atf4*$^{\Delta EC/\Delta EC}$ mice with or without exercise. DNAse treated slides were used as positive control. Scale bar, 100 µm. (**E**) Fiber type composition of WT and *Atf4*$^{\Delta EC/\Delta EC}$ mice with or without exercise (n=6). (**F, G, H**) Representative images of Western Blot (F) and quantification (G, H) of glycolytic and oxidative enzymes in WT and *Atf4*$^{\Delta EC/\Delta EC}$ mice with or without exercise (n=7). (**I**) Gating strategy and analysis of mTomato or mGFP ECs combined with EdU isolated from *Pdgfb-Cre*^{ERT2} x *Rosa26*^{mTmG} control (WT) and *Pdgfb-Cre*^{ERT2} x *Atf4*$^{fl/fl}$ x *Rosa26*^{mTmG} mice (low dose tamoxifen injected) with or without exercise. (**J**) Quantification of the percentage of mTomato^{+} and mGFP^{+} ECs in total ECs (n=3-4) with or without exercise. (**K**) Quantification of percentage of EdU^{+} ECs within mTomato^{+} and mGFP^{+} EC populations (n=3-6) with or without exercise. One-way ANOVA with Tukey's multiple comparisons test in **A** (*p<0.05). Two-way ANOVA with Sidak's multiple comparisons test in **B, C, E, G, H, J, K** (*p<0.05). n.s.: not significant. Each dot represents a single mouse (**A, B, C, E, G, H, J, K**). Bar graphs represent mean ± SEM.